

RESEARCH ARTICLE

# A Novel Genome-Wide Association Study Approach Using Genotyping by Exome Sequencing Leads to the Identification of a Primary Open Angle Glaucoma Associated Inversion Disrupting *ADAMTS17*

Oliver P. Forman<sup>1\*</sup>, Louise Pettitt<sup>1</sup>, András M. Komáromy<sup>3</sup>, Peter Bedford<sup>2</sup>, Cathryn Mellersh<sup>1</sup>

**1** Kennel Club Genetics Centre, Animal Health Trust, Newmarket Suffolk, CB8 7UU, United Kingdom, **2** Department of Clinical Science & Services, Royal Veterinary College, University of London, Hawkshead Lane, Hatfield, Hertfordshire, AL9 7TA, United Kingdom, **3** Department of Small Animal Clinical Sciences, College of Veterinary Medicine, Michigan State University, Veterinary Medical Center, 736 Wilson Road, East Lansing, MI, 48824–1314, United States of America

\* [oliver.forman@aht.org.uk](mailto:oliver.forman@aht.org.uk)



**OPEN ACCESS**

**Citation:** Forman OP, Pettitt L, Komáromy AM, Bedford P, Mellersh C (2015) A Novel Genome-Wide Association Study Approach Using Genotyping by Exome Sequencing Leads to the Identification of a Primary Open Angle Glaucoma Associated Inversion Disrupting *ADAMTS17*. *PLoS ONE* 10(12): e0143546. doi:10.1371/journal.pone.0143546

**Editor:** Degui Zhi, University of Alabama at Birmingham, UNITED STATES

**Received:** September 18, 2015

**Accepted:** October 7, 2015

**Published:** December 18, 2015

**Copyright:** © 2015 Forman et al. This is an open access article distributed under the terms of the [Creative Commons Attribution License](https://creativecommons.org/licenses/by/4.0/), which permits unrestricted use, distribution, and reproduction in any medium, provided the original author and source are credited.

**Data Availability Statement:** Genome sequencing data can be found in the European Nucleotide Archive, study accession number PRJEB11835.

**Funding:** The study into primary open angle glaucoma was funded by the Waltham Foundation ([www.waltham.com/waltham-research/funding-opportunities/](http://www.waltham.com/waltham-research/funding-opportunities/)). The funders had no role in study design, data collection and analysis, decision to publish, or preparation of the manuscript.

## Abstract

Closed breeding populations in the dog in conjunction with advances in gene mapping and sequencing techniques facilitate mapping of autosomal recessive diseases and identification of novel disease-causing variants, often using unorthodox experimental designs. In our investigation we demonstrate successful mapping of the locus for primary open angle glaucoma in the Petit Basset Griffon Vendéen dog breed with 12 cases and 12 controls, using a novel genotyping by exome sequencing approach. The resulting genome-wide association signal was followed up by genome sequencing of an individual case, leading to the identification of an inversion with a breakpoint disrupting the *ADAMTS17* gene. Genotyping of additional controls and expression analysis provide strong evidence that the inversion is disease causing. Evidence of cryptic splicing resulting in novel exon transcription as a consequence of the inversion in *ADAMTS17* is identified through RNAseq experiments. This investigation demonstrates how a novel genotyping by exome sequencing approach can be used to map an autosomal recessive disorder in the dog, with the use of genome sequencing to facilitate identification of a disease-associated variant.

## Introduction

It is well documented that population structure in the purebred dog can help to facilitate genome-wide association study (GWAS) approaches [1]. The development of most modern breeds within the last 200 years from small numbers of founding individuals has led to high levels of linkage disequilibrium (LD) within breeds. These high levels of LD lead to very strong

**Competing Interests:** The authors have declared that no competing interests exist.

signals of association being produced from GWASs for autosomal recessive diseases, even with very modest sample numbers [2]. Closed breeding populations, high levels of inbreeding and the extensive use of popular sires (dogs that closely fit the standard for a particular breed) can lead to rapidly emerging autosomal recessive disorders, as rare deleterious alleles are rapidly amplified. An example of an emerging autosomal recessive disorder is primary open angle glaucoma (POAG) in the Petit Basset Griffon Vendéen (PBGV).

The first recognised case of POAG in the PBGV was identified in the United Kingdom in 1996 and recent survey work completed in 2014 has demonstrated a 10.4% prevalence for the disease (personal communication, Peter Bedford). The initial clinical features of POAG are usually seen in 3 to 4 year old dogs of either sex, the disease being characterised by a small, sustained rise in intraocular pressure (IOP) and lens subluxation. In approximately one third of affected dogs phacodonesis and the appearance of the aphakic crescent associated with lens subluxation are seen before a noticeable rise in IOP (Fig 1). There is no pectinate ligament abnormality and the iridocorneal angle remains open until the late stages of the disease, when globe enlargement has developed. Retinal degeneration and a cupping deformation of the optic papilla are only seen in late disease. Pain is not a feature and the quiet, chronic clinical nature of this disease means that often owners only become aware of the presence of POAG when either the globe enlargement or a vision problem becomes noticeable.

As POAG is an autosomal recessively inherited disease, mapping of which are facilitated by the high levels of LD described, we designed a novel GWAS approach using genotyping by



**Fig 1. POAG case eye image.** Left eye, 4 year old male PBGV: The eye is normotensive (18 mm. Hg.), but an aphakic crescent indicating lens subluxation is visible within the dorsal part of the dilated pupillary aperture.

doi:10.1371/journal.pone.0143546.g001

exome sequencing methodology with 12 cases and 12 controls with the dual aim of identifying both the disease-associated locus and causal variant for POAG through a single experiment.

## Results

### Genome-wide association study by exome sequencing (POAG)

Exome sequencing was carried out using a commercially available human exome capture kit to capture the exomes of 12 POAG cases and 12 breed matched control dogs. Illumina sequencing produced a 15.0 Gb dataset of 250 bp paired-end reads (sufficient for low coverage of ~5x). Alignment to the canine reference sequence CanFam3.1 and variant calling across all 24 individuals identified a total of 841,115 SNP and indel calls (variants). After filtering variants with a minor allele frequency (MAF) of less than 5% and genotyping frequency (GF) of less than 80%, 61,977 remained.

Basic allele association analysis identified a single signal of genome-wide significance on canine chromosome 3 ( $p_{\text{raw}} = 6.15 \times 10^{-10}$ ) (Fig 2). The genomic inflation factor (based on median chi-squared) was 1.34. Correction for the effects of population substructure was performed using a mixed model approach (EMMAX) [3] and the strong single signal on chromosome 3 remained ( $p = 1.34 \times 10^{-9}$ ) (S1 Fig). The adjusted genomic inflation factor (based on median chi-squared) was 1.04.

Visual analysis of the raw genotyping data revealed a disease associated interval of chr3:40,153,292–47,300,360 based on the CanFam3.1 genome build (Fig 3). All cases were homozygous for the disease-associated haplotype. The disease-associated interval contained 28

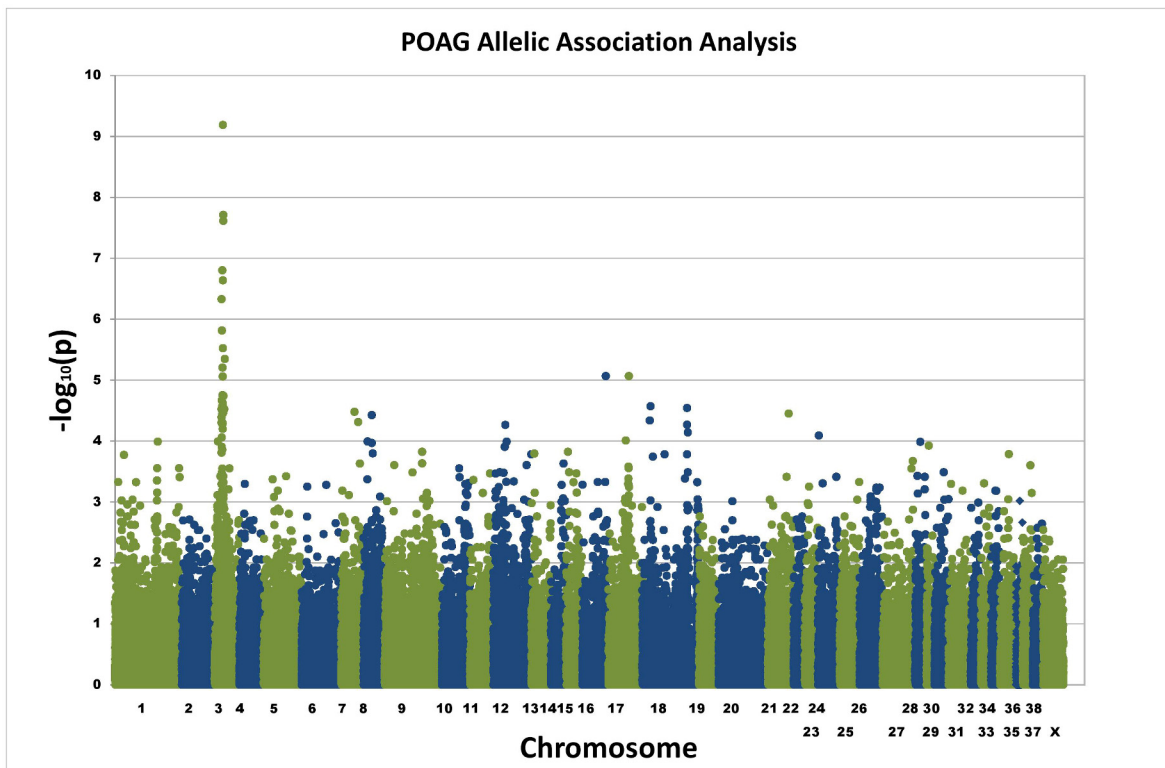


**Fig 2. Allelic association plot for POAG GWAS.** Exome sequencing was used to generate SNPs for 12 POAG cases and 12 controls. Allelic association analysis identified a single signal on chromosome 3 of genome-wide significance.

doi:10.1371/journal.pone.0143546.g002



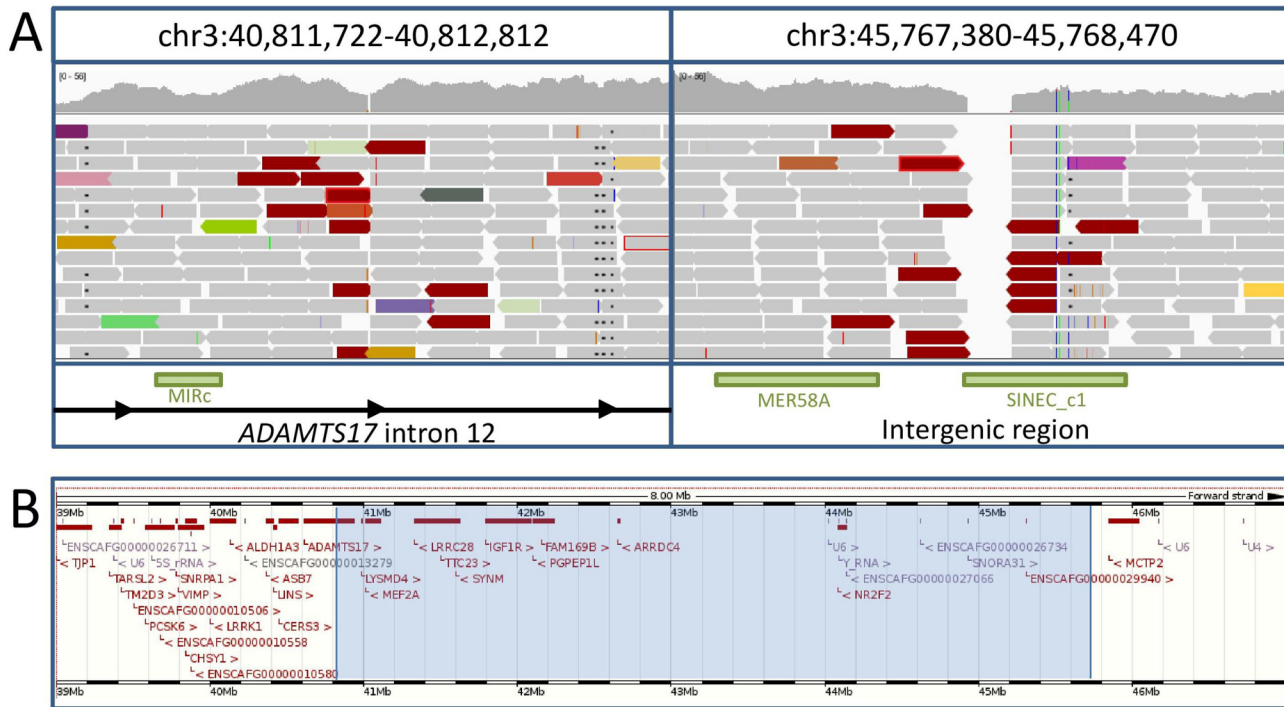


**Fig 4. The POAG associated inversion.** (A) Reads aligning across the inversion breakpoints. Red reads indicate a greater than expected insert size. Read mates for red reads align in the same direction, indicative of an inversion. There were five deleted bases at the 5' inversion breakpoint and 78 deleted bases at the 3' deletion breakpoint. Green boxes indicate repeat elements. (B) Overview of the genomic region covered by the inversion. The inverted region is highlighted in blue. Genotyping of the inversion was carried out to confirm the association with POAG. A total of 225 PBGVs were genotyped, including 28 POAG cases, of which 27 were homozygous for the inversion. Results are summarised in [Table 1](#).

doi:10.1371/journal.pone.0143546.g004

suitable case and control material and assessment of expression levels of *ADAMTS17* using RNAseq data generated in previous studies (data not shown). In a comparison of retinal cDNA from one POAG case against one control, results suggested a 2.4 fold increase in *ADAMTS17* expression upstream of the inversion for the POAG case relative to the control. No *ADAMTS17* expression was detected downstream of the inversion for the POAG case. (Full results are shown in [S1 Dataset](#)).

RNAseq data generated from retinal RNA of one POAG case, showed concordance with the results of qPCR analysis. Expression of novel exons as the result of cryptic splicing was observed after the final normally transcribed exon of *ADAMTS17* before disruption by the inversion. An example of a novel exon established through a cryptic splicing event is shown in [Fig 5](#). A schematic diagram of *ADAMTS17* exon arrangement is shown in [Fig 6](#).

**Table 1. Genotyping of an extended PBGV sample set for the POAG-associated inversion.**

	+/+	INV/+	INV/INV
POAG cases	1	0	48
controls	92	71	0
<b>TOTALS</b>	<b>93</b>	<b>71</b>	<b>48</b>

Results of genotyping 212 PBGV for the POAG associated inversion, where + represents the reference allele and INV represents the inversion allele.

doi:10.1371/journal.pone.0143546.t001

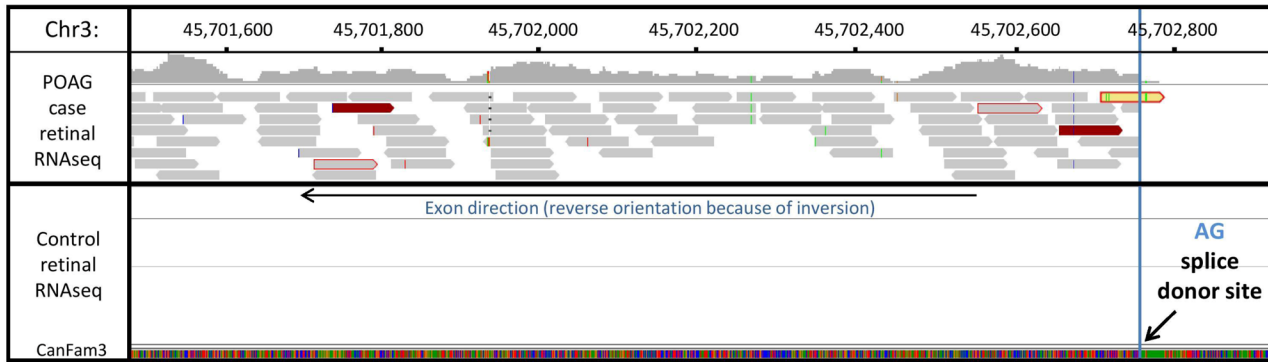


**Fig 5. Example of novel exon formation through cryptic splicing.** An example of a novel exon occurring due to a cryptic splicing event visualised through aligned RNAseq reads. A splice donor site and reads spanning to the previous exon (solid red) can be identified. There are no reads aligning to the region for the control individual (lower panel).

doi:10.1371/journal.pone.0143546.g005

Both of the sequences of the two independent novel exons contained stop codons after an aberrant sequence of amino acids (S1 File).

### Discussion

In this investigation we have demonstrated a novel GWAS approach using exome sequencing variants calls as the genotyping dataset. The major potential advantage of this approach is that a causal variant for a single gene disease could be identified in a single step, and would theoretically be the most strongly disease segregating variant with the lowest associated p-value (top SNP). Although the causal variant for POAG was not directly found by this method, due to the non-exonic location, a genome-wide significant locus was identified, enabling a disease-associated interval to be determined.

The causal mutation for POAG was eventually identified through a genome sequencing approach. Genome sequencing is an increasingly cost effective method of following up disease-associated intervals identified through GWAS. In contrast to other approaches such as exome sequencing and target enrichment, coverage is near to 100%, enabling identification of causal mutations in repetitive regions of the genome. Genome sequencing has recently been adopted to directly identify causal mutations in the dog [5–7] and is being used in human studies through projects such as the 100,000 genomes project, studying cancers and rare diseases [8]. However, structural variants still often present a challenge to smaller laboratories using

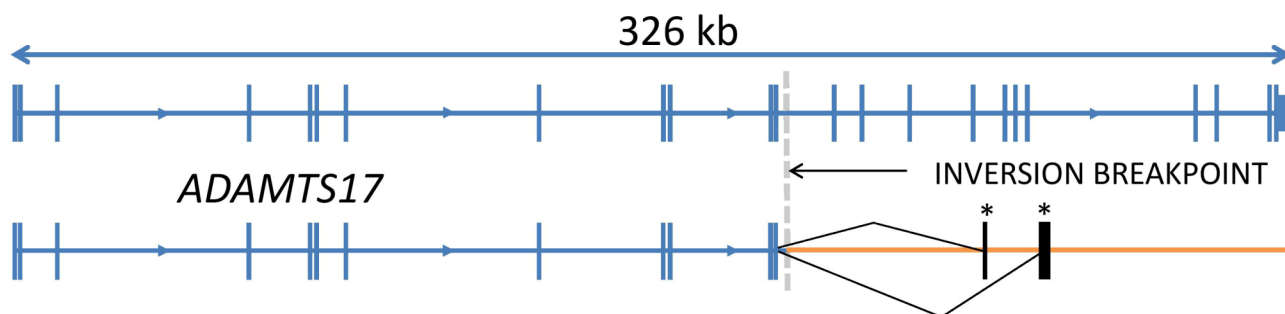


**Fig 6. Schematic gene arrangements for the reference and inversion alleles.** Transcript arrangements for the *ADAMTS17* reference gene and *ADAMTS17* after the inversion event. Novel exons are marked with an asterisk.

doi:10.1371/journal.pone.0143546.g006

genome sequencing as part of an investigation, making GWAS in many cases the most appropriate method of locus identification for single gene diseases, before using genome sequencing or other approaches to interrogate disease-associated intervals.

Although the *ADAMTS17* gene was majorly disrupted by the inversion, qPCR analysis on a limited number of samples showed little evidence of nonsense mediated decay, as expression of exons outside of the inverted region was not majorly affected. Analysis of RNAseq data revealed novel exon expression for *ADAMTS17* due to cryptic splicing occurring 3' of the exons located immediately upstream of the inversion event. The unavailability of suitable antibodies targeting the 5' region of *ADAMTS17* prevented western blot analysis to determine whether protein is still produced from the modified transcript sequence. Visual analysis of RNAseq data aligned to the genes flanking and within the inversion region suggested gene expression for these genes was not affected. We speculate that a mobile element (SINE) which spans the 3' inversion breakpoint is likely to have been involved in the inversion mechanism, although there is no similar mobile element in the 5' region. There is one previous report of a gene rearrangement involving *ADAMTS17* found in a patient with pregnancy-related acute promyelocytic leukemia [9]. This rearrangement resulted in a novel transcription product with the insertion of exon 15 of *ADAMTS17* between the PML and RARA genes. As the breakpoint within *ADAMTS17* identified in this study was within intron 12, it is unlikely that the mutation mechanism was shared between these two independent events.

Genotyping of an extended sample set was used to determine whether the identified inversion was fully concordant with POAG. Of the 212 PBGV assayed for the POAG associated inversion there was one discordant case. A single dog was reported as having clinical signs of POAG but was homozygous for the reference sequence. It could be speculated that POAG for this case is due to another clinical or genetic cause, or is a secondary form of glaucoma.

A Weill-Marchesani like syndrome (WMS) in humans was the first disease phenotype to be associated with mutations in the *ADAMTS17* gene. Clinical signs of WMS include glaucoma, ectopia lentis (lens luxation), lenticular myopia, spherophakia, and short stature [10]. It is interesting to speculate that as the PBGV is a miniature version of the Grand Basset Griffon Vendéen, artificial selection pressure for small size may have contributed to an increase in mutant allele frequency, assuming mutations in *ADAMTS17* could be contributing to small stature. An *ADAMTS17* splice donor site mutation has been associated with hereditary primary lens luxation in several breeds of dog [11, 12]. The range of phenotypes associated with *ADAMTS17* mutations suggests that the exact phenotypic presentation is dependent on the positioning and nature of the mutations within the *ADAMTS17* gene. The *ADAMTS17* gene is a member of the ADAMTS family of extracellular proteases [13]. Domains which are characteristic of the ADAMTS family include an N terminal protease domain and a C-terminal ancillary domain [14]. The inversion in intron 12 of *ADAMTS17* is within the proteolytic domain and is therefore likely to disrupt the enzymatic function of the protein. Phenotypic similarities between ADAMTS associated disease and Fibrillin1 (*FBN1*) associated disease, and functional evidence, suggest ADAMTS family members have a role in microfibril assembly and function [15]. It could be speculated that disruption of the maintenance of microfibrils in the eye are likely to lead to development of disease phenotypes such as lens luxation and glaucoma [16]. The role of the ADAMTS family members in glaucoma pathogenesis is further highlighted by the identification of a mutation in *ADAMTS10* as the cause of glaucoma in the Beagle and Norwegian Elkhound dog breeds [17, 18]. Functional work would be required to further understand the roles of the ADAMTS family in glaucoma disease pathogenesis.

In summary, we have used a novel GWAS approach and genome sequencing to identify an inversion associated with POAG in the PBGV dog breed. The approach further highlights how

the increasing availability and cost effectiveness of massively parallel sequencing are facilitating studies into inherited disease in the dog.

## Materials and Methods

### Ethics Statement

Collection of DNA samples was performed by buccal swabbing, which is a non-invasive technique that does not require a United Kingdom Home Office License. Only pet dogs were used in the study with full owner consent. Tissue samples for the study into primary open angle glaucoma were obtained after enucleation of a glaucoma case by a veterinary ophthalmologist on welfare grounds due to the severity of clinical signs (carried out in accordance with the Veterinary Surgeons Act 1966 and under the auspices of the RCVS). Full owner consent was obtained. As the techniques used were either non-invasive or in the case of eye surgery, were required to alleviate animal suffering rather than for research purposes, no ethics committee approval was required.

### Diagnosis of POAG cases, and sample set selection

All cases of POAG were diagnosed by a specialist veterinary ophthalmologist. The basic clinical examination for POAG involves the use of slit lamp biomicroscopy, both indirect and direct ophthalmoscopy, applanation tonometry and gonioscopy. Tonometry and gonioscopy are completed before inducing mydriasis using 1% tropicamide, slit lamp biomicroscopy utilised pre and post mydriasis and ophthalmoscopy post mydriasis. Vision assessment is based on history, the menace and dazzle reflexes and, where possible, maze performance.

### DNA extraction and genotyping

DNA was extracted from buccal swabs using the QIAamp Midi kit (Qiagen). Genotyping of the POAG associated inversion was performed by analysis of a fragment length polymorphism generated by PCR. Primers for PCR were as follows: POAG\_F, 6FAM-AGGCTCAGAGGAGGGTGACT; POAG\_R1, ACAAGGACAAAGCTGTCTGTGA; POAG\_R2, ACACAAAGCACCCATGACAG. PCRs were carried out in 12 ul volumes consisting of 1.5 mM dNTPs, 1x Qiagen PCR buffer, 0.5 μM of each primer, 0.6U of Qiagen HotStarTaq polymerase and template DNA. Thermal cycling consisted of 5 minutes at 95°C, followed by 35 cycles of 95°C for 30 seconds, 57°C for 30 seconds, and 72°C for 30 seconds, with a final elongation stage of 72°C for 5 minutes. Products of PCR were analysed using the fragment analysis module of an ABI3130xl genetic analyser. Sequencing of the *ADAMTS17* gene was carried out as previously described [11].

### Exome sequencing and allelic association analysis

Libraries for exome sequencing of 12 POAG cases and 12 breed matched controls were made using the Illumina Nextera Exome Enrichment kit according to the manufacturer's instructions. Libraries were quantified by qPCR using the KAPA library quantification kit. Sequencing of libraries was performed using two runs on the Illumina MiSeq platform, generating paired-end reads of 250 bp in length. The sequence reads generated were aligned to the canine reference genome build, CanFam3.1 using BWA [19]. Variants were called using the GATK [20]. Variants were converted to PLINK format for use in allelic association analysis using VCFtools [21]. Allelic association analyses were carried out using the whole genome data analysis toolset, PLINK [22]. Genome sequencing was outsourced to the Wellcome Trust Centre for Human

Genetics, Oxford. Sequencing data can be found in the European Nucleotide Archive, study accession number PRJEB11835.

## Expression analysis

RNA was extracted from retina using the Qiagen RNeasy Midi kit, and included an on column DNase treatment. Isolation of mRNA from total RNA was performed using Sera-Mag oligo-dT beads. Libraries for RNAseq were generated using NEBNext Ultra RNA Library Prep Kit for Illumina sequencing. Sequencing was performed on an Illumina MiSeq generating a dataset of 75 bp paired-end reads, using one run per RNAseq library. Approximate dataset sizes were 4 Gb.

Synthesis of cDNA for qPCR expression analysis was performed using the Qiagen QuantiTect reverse transcription kit. Expression analysis by qPCR was performed in 8  $\mu$ l reactions, containing 1x primer-probe mix, 1x KAPA Probe Fast qPCR Master Mix and 2  $\mu$ l template cDNA. Standard curves were generated over a seven point, two fold dilution. Standard curves for all qPCR assays had an  $r^2$  of greater than 0.99 and all assays had an efficiency of greater than 95%. Primers for qPCR, reaction efficiencies and full datasets with calculations can be found in [S1 Dataset](#).

## Supporting Information

**S1 Dataset. qRT-PCR primer sequences, reaction efficiencies and calculations.**

(XLSX)

**S1 Fig. Association analysis using a Mixed Model approach correcting for population structure for the POAG GWAS.**

(TIF)

**S1 File. Sequence information for novel ADAMTS17 exons.**

(DOCX)

**S1 Table. Genes in the disease-associated interval for POAG.**

(DOCX)

**S2 Table. Non-synonymous SNP variants in the POAG disease-associated interval.**

(DOCX)

## Acknowledgments

We are thankful to all owners, breeders and clinicians that have contributed samples to this study. We thank the High-Throughput Genomics Group at the Wellcome Trust Centre for Human Genetics for the generation of the sequencing data.

## Author Contributions

Conceived and designed the experiments: OPF CM. Performed the experiments: OPF LP. Analyzed the data: OPF. Contributed reagents/materials/analysis tools: OPF AMK PB CM. Wrote the paper: OPF LP AMK PB CM.

## References

1. Parker HG, Kukekova AV, Akey DT, Goldstein O, Kirkness EF, Baysac KC, et al. Breed relationships facilitate fine-mapping studies: a 7.8-kb deletion cosegregates with Collie eye anomaly across multiple dog breeds. *Genome research*. 2007; 17(11):1562–71. doi: [10.1101/gr.6772807](https://doi.org/10.1101/gr.6772807) PMID: [17916641](https://pubmed.ncbi.nlm.nih.gov/17916641/); PubMed Central PMCID: PMC2045139.

2. Safra N, Bassuk AG, Ferguson PJ, Aguilar M, Coulson RL, Thomas N, et al. Genome-wide association mapping in dogs enables identification of the homeobox gene, NKX2-8, as a genetic component of neural tube defects in humans. *PLoS Genet.* 2013; 9(7):e1003646. doi: [10.1371/journal.pgen.1003646](https://doi.org/10.1371/journal.pgen.1003646) PMID: [23874236](https://pubmed.ncbi.nlm.nih.gov/23874236/); PubMed Central PMCID: PMC3715436.
3. Kang HM, Sul JH, Service SK, Zaitlen NA, Kong SY, Freimer NB, et al. Variance component model to account for sample structure in genome-wide association studies. *Nat Genet.* 2010; 42(4):348–54. doi: [10.1038/ng.548](https://doi.org/10.1038/ng.548) PMID: [20208533](https://pubmed.ncbi.nlm.nih.gov/20208533/); PubMed Central PMCID: PMC3092069.
4. Robinson JT, Thorvaldsdottir H, Winckler W, Guttman M, Lander ES, Getz G, et al. Integrative genomics viewer. *Nat Biotechnol.* 2011; 29(1):24–6. doi: [10.1038/nbt.1754](https://doi.org/10.1038/nbt.1754) PMID: [21221095](https://pubmed.ncbi.nlm.nih.gov/21221095/); PubMed Central PMCID: PMC3346182.
5. Gilliam D, O'Brien DP, Coates JR, Johnson GS, Johnson GC, Mhlanga-Mutangadura T, et al. A homozygous KCNJ10 mutation in Jack Russell Terriers and related breeds with spinocerebellar ataxia with myokymia, seizures, or both. *Journal of veterinary internal medicine / American College of Veterinary Internal Medicine.* 2014; 28(3):871–7. doi: [10.1111/jvim.12355](https://doi.org/10.1111/jvim.12355) PMID: [24708069](https://pubmed.ncbi.nlm.nih.gov/24708069/); PubMed Central PMCID: PMC4238845.
6. Guo J, Johnson GS, Brown HA, Provencher ML, da Costa RC, Mhlanga-Mutangadura T, et al. A CLN8 nonsense mutation in the whole genome sequence of a mixed breed dog with neuronal ceroid lipofuscinosis and Australian Shepherd ancestry. *Molecular genetics and metabolism.* 2014; 112(4):302–9. doi: [10.1016/j.ymgme.2014.05.014](https://doi.org/10.1016/j.ymgme.2014.05.014) PMID: [24953404](https://pubmed.ncbi.nlm.nih.gov/24953404/).
7. Guo J, O'Brien DP, Mhlanga-Mutangadura T, Olby NJ, Taylor JF, Schnabel RD, et al. A rare homozygous MFSD8 single-base-pair deletion and frameshift in the whole genome sequence of a Chinese Crested dog with neuronal ceroid lipofuscinosis. *BMC veterinary research.* 2014; 10:960. doi: [10.1186/s12917-014-0181-z](https://doi.org/10.1186/s12917-014-0181-z) PMID: [25551667](https://pubmed.ncbi.nlm.nih.gov/25551667/); PubMed Central PMCID: PMC4298050.
8. Siva N. UK gears up to decode 100,000 genomes from NHS patients. *Lancet.* 2015; 385(9963):103–4. doi: [10.1016/S0140-6736\(14\)62453-3](https://doi.org/10.1016/S0140-6736(14)62453-3) PMID: [25540888](https://pubmed.ncbi.nlm.nih.gov/25540888/).
9. Lim G, Cho EH, Cho SY, Shin SY, Park JC, Yang YJ, et al. A novel PML-ADAMTS17-RARA gene rearrangement in a patient with pregnancy-related acute promyelocytic leukemia. *Leukemia research.* 2011; 35(7):e106–10. doi: [10.1016/j.leukres.2011.03.020](https://doi.org/10.1016/j.leukres.2011.03.020) PMID: [21529941](https://pubmed.ncbi.nlm.nih.gov/21529941/).
10. Morales J, Al-Sharif L, Khalil DS, Shinwari JM, Bavi P, Al-Mahrouqi RA, et al. Homozygous mutations in ADAMTS10 and ADAMTS17 cause lenticular myopia, ectopia lentis, glaucoma, spherophakia, and short stature. *Am J Hum Genet.* 2009; 85(5):558–68. doi: [10.1016/j.ajhg.2009.09.011](https://doi.org/10.1016/j.ajhg.2009.09.011) PMID: [19836009](https://pubmed.ncbi.nlm.nih.gov/19836009/); PubMed Central PMCID: PMC2775842.
11. Farias FH, Johnson GS, Taylor JF, Giuliano E, Katz ML, Sanders DN, et al. An ADAMTS17 splice donor site mutation in dogs with primary lens luxation. *Invest Ophthalmol Vis Sci.* 2010; 51(9):4716–21. Epub 2010/04/09. iovs.09-5142 [pii] doi: [10.1167/iovs.09-5142](https://doi.org/10.1167/iovs.09-5142) PMID: [20375329](https://pubmed.ncbi.nlm.nih.gov/20375329/).
12. Gould D, Pettitt L, McLaughlin B, Holmes N, Forman O, Thomas A, et al. ADAMTS17 mutation associated with primary lens luxation is widespread among breeds. *Vet Ophthalmol.* 2011; 14(6):378–84. doi: [10.1111/j.1463-5224.2011.00892.x](https://doi.org/10.1111/j.1463-5224.2011.00892.x) PMID: [22050825](https://pubmed.ncbi.nlm.nih.gov/22050825/).
13. Porter S, Clark IM, Kevorkian L, Edwards DR. The ADAMTS metalloproteinases. *The Biochemical journal.* 2005; 386(Pt 1):15–27. doi: [10.1042/BJ20040424](https://doi.org/10.1042/BJ20040424) PMID: [15554875](https://pubmed.ncbi.nlm.nih.gov/15554875/); PubMed Central PMCID: PMC1134762.
14. Mosyak L, Georgiadis K, Shane T, Svenson K, Hebert T, McDonagh T, et al. Crystal structures of the two major aggrecan degrading enzymes, ADAMTS4 and ADAMTS5. *Protein science: a publication of the Protein Society.* 2008; 17(1):16–21. doi: [10.1110/ps.073287008](https://doi.org/10.1110/ps.073287008) PMID: [18042673](https://pubmed.ncbi.nlm.nih.gov/18042673/); PubMed Central PMCID: PMC2144589.
15. Hubmacher D, Apte SS. Genetic and functional linkage between ADAMTS superfamily proteins and fibrillin-1: a novel mechanism influencing microfibril assembly and function. *Cellular and molecular life sciences: CMLS.* 2011; 68(19):3137–48. doi: [10.1007/s00018-011-0780-9](https://doi.org/10.1007/s00018-011-0780-9) PMID: [21858451](https://pubmed.ncbi.nlm.nih.gov/21858451/).
16. Kuchtey J, Kuchtey RW. The microfibril hypothesis of glaucoma: implications for treatment of elevated intraocular pressure. *Journal of ocular pharmacology and therapeutics: the official journal of the Association for Ocular Pharmacology and Therapeutics.* 2014; 30(2–3):170–80. doi: [10.1089/jop.2013.0184](https://doi.org/10.1089/jop.2013.0184) PMID: [24521159](https://pubmed.ncbi.nlm.nih.gov/24521159/); PubMed Central PMCID: PMC3991966.
17. Kuchtey J, Olson LM, Rinkoski T, Mackay EO, Iverson TM, Gelatt KN, et al. Mapping of the disease locus and identification of ADAMTS10 as a candidate gene in a canine model of primary open angle glaucoma. *PLoS Genet.* 2011; 7(2):e1001306. doi: [10.1371/journal.pgen.1001306](https://doi.org/10.1371/journal.pgen.1001306) PMID: [21379321](https://pubmed.ncbi.nlm.nih.gov/21379321/); PubMed Central PMCID: PMC3040645.
18. Ahonen SJ, Kaukonen M, Nussdorfer FD, Harman CD, Komaromy AM, Lohi H. A novel missense mutation in ADAMTS10 in Norwegian Elkhound primary glaucoma. *PLoS One.* 2014; 9(11):e111941. doi: [10.1371/journal.pone.0111941](https://doi.org/10.1371/journal.pone.0111941) PMID: [25372548](https://pubmed.ncbi.nlm.nih.gov/25372548/); PubMed Central PMCID: PMC4221187.

19. Li H, Durbin R. Fast and accurate short read alignment with Burrows-Wheeler transform. *Bioinformatics*. 2009; 25(14):1754–60. Epub 2009/05/20. btp324 [pii] doi: [10.1093/bioinformatics/btp324](https://doi.org/10.1093/bioinformatics/btp324) PMID: [19451168](https://pubmed.ncbi.nlm.nih.gov/19451168/); PubMed Central PMCID: PMC2705234.
20. McKenna A, Hanna M, Banks E, Sivachenko A, Cibulskis K, Kernytsky A, et al. The Genome Analysis Toolkit: a MapReduce framework for analyzing next-generation DNA sequencing data. *Genome Res*. 2010; 20(9):1297–303. Epub 2010/07/21. gr.107524.110 [pii] doi: [10.1101/gr.107524.110](https://doi.org/10.1101/gr.107524.110) PMID: [20644199](https://pubmed.ncbi.nlm.nih.gov/20644199/); PubMed Central PMCID: PMC2928508.
21. Danecek P, Auton A, Abecasis G, Albers CA, Banks E, DePristo MA, et al. The variant call format and VCFtools. *Bioinformatics*. 2011; 27(15):2156–8. doi: [10.1093/bioinformatics/btr330](https://doi.org/10.1093/bioinformatics/btr330) PMID: [21653522](https://pubmed.ncbi.nlm.nih.gov/21653522/); PubMed Central PMCID: PMC3137218.
22. Purcell S, Neale B, Todd-Brown K, Thomas L, Ferreira MA, Bender D, et al. PLINK: a tool set for whole-genome association and population-based linkage analyses. *American journal of human genetics*. 2007; 81(3):559–75. doi: [10.1086/519795](https://doi.org/10.1086/519795) PMID: [17701901](https://pubmed.ncbi.nlm.nih.gov/17701901/); PubMed Central PMCID: PMC1950838.